Deep-Level Optically Addressable Defects: Transition Metals in ZnS and MgO

Abdul Muhaymin,[1,*] and Cüneyt Şahin[1]

[1]UNAM - National Nanotechnology Research Center, Institute of Materials Science and Nanotechnology, Bilkent University, Ankara, Turkey.

[*]abdul.muhaymin@bilkent.edu.tr

17th NanoDay'25, 2025, May 23, Friday, UNAM CONFERENCE HALL

Introduction & Motivation

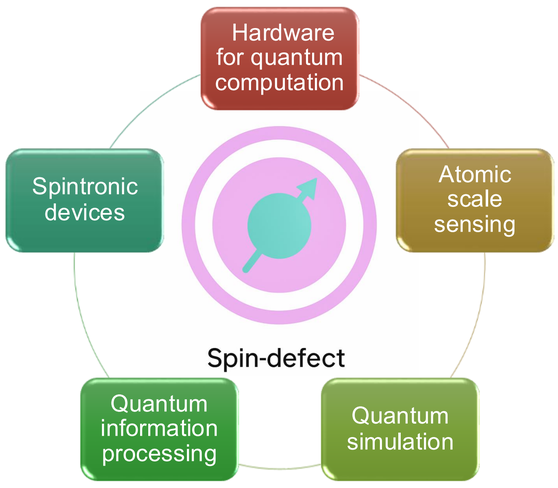

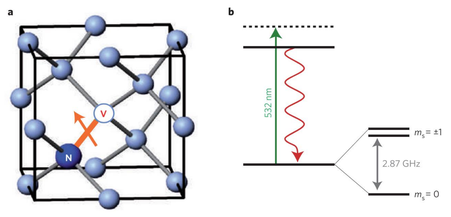

Figure 1: Crystal structure of the NV-center in diamond, a widely studied single defect material, shown with its energy level [1]

Our overarching goal is to systematically study **various transition metal (TM) -related defect** in **different host materials** to determine the best performing combination. Towards this goal, here we report our study on the **substitutional X** and nearest neighbor (NN) **X-vacancy** centers in **ZnS** and **MgO** where **X = Cu, Co, Ni, Fe.**

Methodology

We performed first-principles plane-wave based spin-polarized Density Functional Theory (DFT) calculations using the Perdew-Burke-Ernzerhof (PBE) exchange and correlation functionals as implemented in the Quantum ESPRESSO code [2]. We used a scalar relativistic Projector Augmented Wave (PAW) pseudopotential with non-linear core correction.

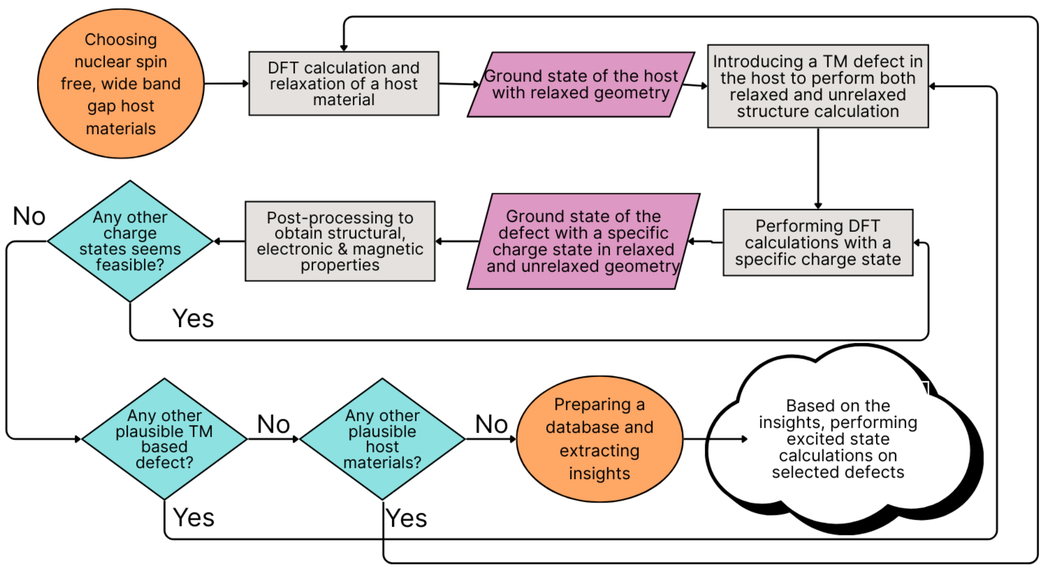

Figure 2: The workflow of this study.

Following our calculation, we have extracted:

- Structural properties
- Electronic properties
- Magnetic properties
- Defect formation energies [4]

Calculation done on 64 atoms supercell containing 32 **cation (Zn or Mg)** and 32 **anion (S or O)**. So, single TM dopant cation-substitution corresponds to 3.125% of doping concentration which is low enough to capture the physics exhibited by experimental dilute limit doping.

The parameters that were converged before proceeding to any calculations: **(1)** Kinetic energy cutoff (125 Ry - ZnS, 95 Ry - MgO), **(2)** Charge density cutoff (500 Ry - ZnS, 380 Ry - MgO), **(3)** K-point grid density (unshifted, $4 \times 4 \times 4$), **(4)** Lattice parameter (5.442 Å - ZnS, 4.250 Å - MgO), **(5)** Smearing (Gaussian, 0.0001 Ry).

Structural properties of ZnS & MgO and their defect centers

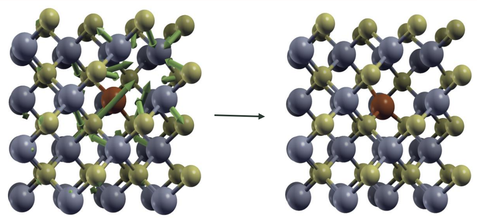

Figure 3: On the left side, an unrelaxed structure is shown where the **green** arrows denote the internal forces on the atoms. On the right side, the structure is relaxed using the BFGS algorithm where the forces becomes negligible.

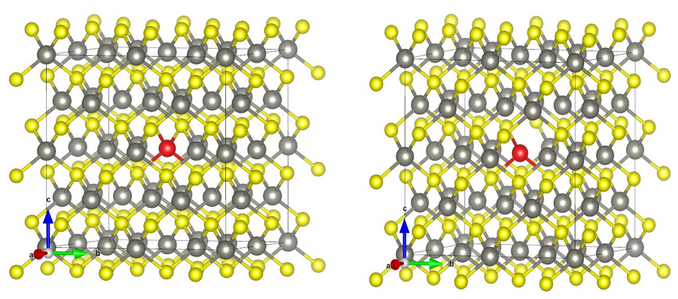

Figure 4: The *zb* ZnS unit cell (left), and the supercell used in this study with a substitutional TM defect (middle) and TM-vacancy center (right).

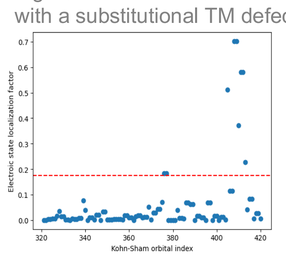

Figure 5: The localization factor analysis shows that only the electronic states contributed by defect complex have the highest localization factor. We can form active space with these defect states that can be treated with higher level of theory and the rest as a dielectric environment [6]

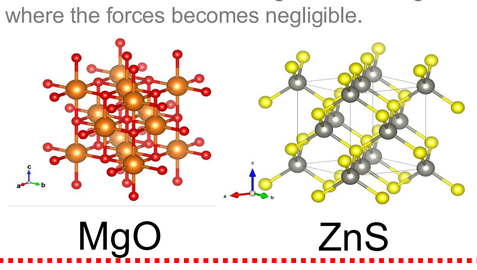

Applications

- **Optically addressable qubits**
- **Dilute magnetic semiconductors**
- **Single-chip computers**
- **Quantum memories**
- **Scalable solid-state quantum sensors**

Storage capability of ferromagnets

Processing power of semiconductors

Spintronics (possible single-chip computer!)

Figure 5: Spintronic can be described as the integration of ferromagnetic storage and semiconducting processors.

Defect screening

For a point defect D, with charge state q, the defect formation energy as a function of Fermi level is given by [3, 4]:

$$E_f^D(q, E_F) = E_{\text{total}}^D - E_{\text{total}}^{\text{Pristine}} + E_{\text{corr}}^q - \sum n_i \mu_i + q(E_F + E_{\text{VBM}}^{\text{Pristine}} + \Delta V_{q/b})$$

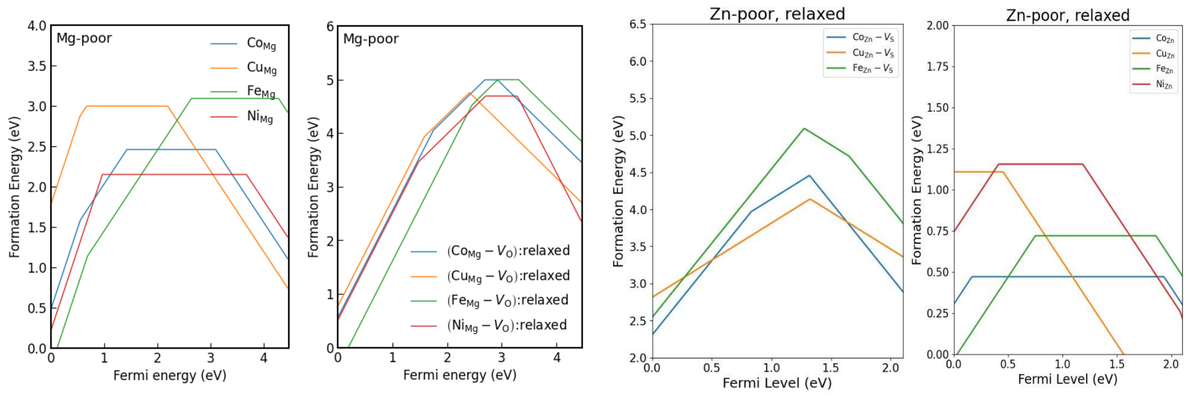

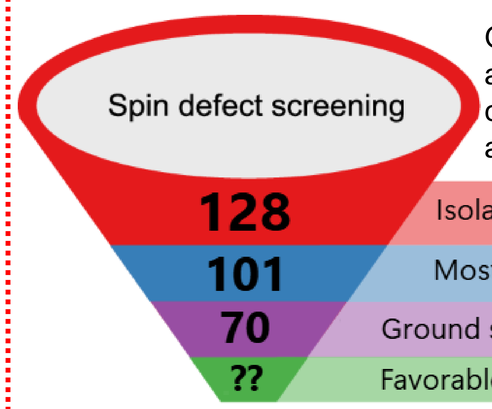

Our calculation successfully screened possible defects, and we can now proceed with expensive optical calculations for only a few selected defects based on their already calculated electronic and magnetic properties

Electronic, magnetic and optical properties

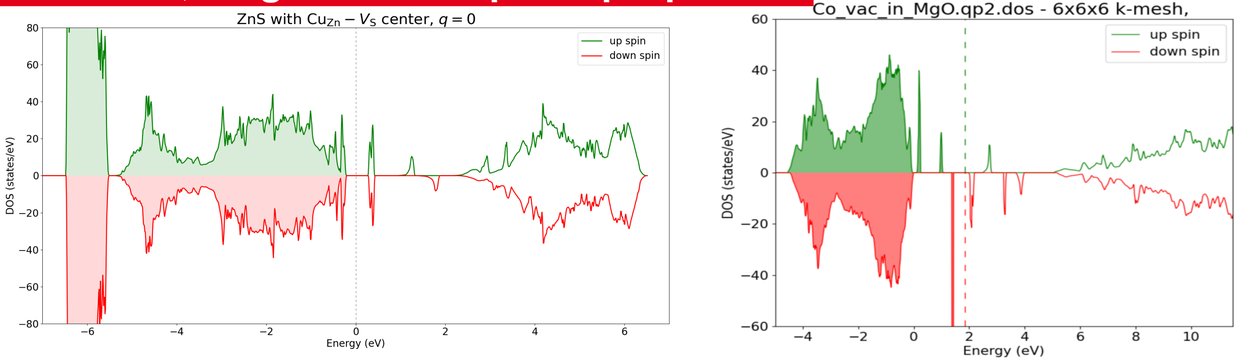

Figure 7: PBE level electronic density of states for Cu-vac center in ZnS with q=0 (left) and Co-vac center in MgO with q=+2 (right).

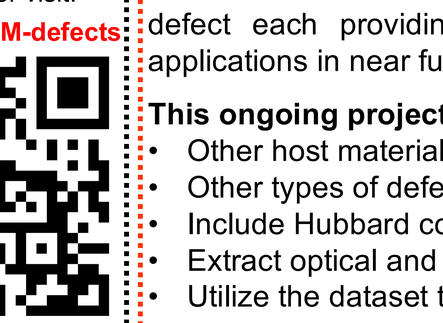

Figure 8: The LDOS clearly shows the localization of electronic states around the defect complex position in Cu-vac center with q=0 in unrelaxed geometry (Blue: UP, red: DOWN spin).

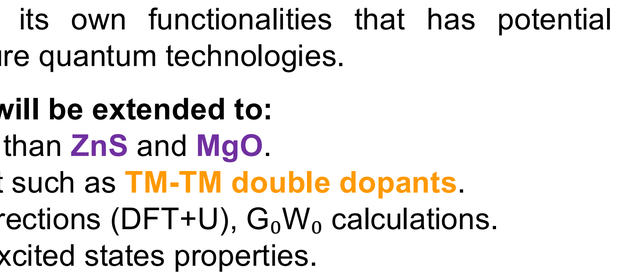

Figure 9: Simulated real and imaginary parts of the dielectric function of MgO using independent particle approximation.

Figure 10: Simulated UV-vis optical absorption spectra of ZnS using Tamm-Dancoff approximation on GW-BSE level.

Band gap	ZnS	MgO
Experimental	3.66 eV	7.70 eV
PBE	2.01 eV	4.47 eV
PBE + U	2.46 eV	-
G_0W_0 @ PBE	3.17 eV	7.16 eV

Table 1: The electronic band gap of the pristine host materials studied. Due to the S-3p states occupying band edges, PBE+U didn't improve the band gap since U was applied on Zn-3d. Even though the semilocal states of Zn makes ZnS harder to treat computationally, we have found the band gap to be within satisfactory limit. For both hosts, we performed GW calculations using WEST code [7].

To see the relaxation animations, and a comprehensive list of visualizations, scan the QR code, or visit:

tinyurl.com/TM-defects

Conclusions & future work

We showed that **TM impurities** as well as NN **TM-vacancy defect complexes** in **ZnS & MgO** can give rise to interesting phenomena. We also showed that there can exist multiple charged states of these defect each providing its own functionalities that has potential applications in near future quantum technologies.

This ongoing project will be extended to:

- Other host materials than **ZnS** and **MgO**.
- Other types of defect such as **TM-TM double dopants**.
- Include Hubbard corrections (DFT+U), G_0W_0 calculations.
- Extract optical and excited states properties.
- Utilize the dataset to train machine learning models.

Supports

unam excellence in science and technology

TÜBİTAK Project No: 123F142

Barcelona Supercomputing Center, Centro Nacional de Supercomputación

References

[1] Koenraad, P. M. & Flatte, M. E. *Nature Mater.,* **10**, 91 (2011)

[2] Giannozzi, P. *et al*., J. Chem. Phys., **152**, 154105 (2020)

[3] Freysoldt, C. *et al*., *Phys. Status Solidi B*, **248**, 1067 (2011)

[4] Thompson, S. M. *et al.*, *ACS Nano*, **17**, 5963 (2023)

[5] Sharma, M. *et al., Phys. Rev. B*, **100**, 045151 (2019)

[6] Sheng *et al., J. Chem. Theory Comput.* **18**, 3512 (2022)

[7] Govoni *et al*., *J. Chem. Theory Comput.* **11**, 2680 (2015)